

Force Propagation in Active Cytoskeletal Networks

Shichen Liu^{1*}, Rosalind Wenshan Pan¹, Heun Jin Lee²,
Shahriar Shadkhoo¹, Fan Yang¹, David Larios¹, Chunhe Li³,
Zijie Qu³, Matt Thomson^{1*}

^{1*}Division of Biology and Biological Engineering, California Institute of Technology, Pasadena, 91125, CA, USA.

²Department of Applied Physics, California Institute of Technology, Pasadena, 91125, CA, USA.

³UM-SJTU Joint Institute, Shanghai Jiao Tong University, Shanghai, 200240, Shanghai, China.

*Corresponding author(s). E-mail(s): slu7@caltech.edu;
mthomson@caltech.edu;

Abstract

In biological systems, energy-consuming active networks of motor and filament proteins generate the forces that drive processes, including motility, shape change, and replication. Despite the integral role of such active material, how molecular-scale interactions can enable the global organization and transmission of forces remains elusive. Here, we demonstrate that the bundling of microtubules can shift motor filament active matter between a global force transmitting phase and a local force dissipating phase. A 5-fold increase in the average microtubule length results in a transition from a local to global phase with a 100-fold increase in the length scale over which forces propagate and a 20-fold increase in force magnitude. The global phase generates (10pN) force fields that enable applications, including cell transport and droplet motility. Through theory and simulation, we demonstrate that even a minority species of long microtubules can induce a percolation transition between a local and global phase, providing a mechanism for the regulation of force transmission in cells. Our results reveal potential mechanisms underlying the propagation of forces in cells and enable the engineering of active materials in synthetic biology and soft robotics.

Introduction

In biological systems, forces are generated at molecular scales by energy-consuming motor and filament proteins within cytoskeletal networks. [1–9]. Molecular-scale forces transmit and amplify through space as proteins consume energy and self-organize into structures up to a million-fold bigger than a single molecule[6, 10–12]. Exactly how the molecular interactions enable force propagation from nanometer to micrometer length scales, however, remains elusive. The mitotic spindle, the cytoskeleton structure that pulls apart chromatids during mitosis, spans from a few microns in yeast to 50 microns in *Xenopus* oocytes and is capable of exerting force pulling chromatids over a few to ten microns. The lamellipodium, a cytoskeletal projection on the leading edge of a cell, spans over tens of micrometers and propagates forces across the leading edge to enable cell motility[11, 13–18]. Force propagation is also apparent in *Drosophila melanogaster* oocytes, where studies of streaming during oocyte development have revealed a transition from a spatially disordered cytoskeleton, supporting flows with only short-ranged correlations, to an ordered state with cell-spanning vortical flow[9, 19–22]. The knowledge gap between how self-organized structure influences force propagation and force dissipation limits our ability to harness these mechanisms in engineering biological and synthetic systems.

Well-controlled reconstituted active cytoskeletal networks allow detailed tests of principles of active matter such as flow generation, nematic bundling, and network contraction and provide a foundation for understanding complex self-organizing processes taking place inside cells. These reconstituted active systems, which convert energy into mechanical work involving microtubules and kinesin motors, form various self-assembled structures from micrometers to millimeters.[23–25] Despite the detailed observations of spatial structures in reconstituted active cytoskeletal networks, the relationship between molecular interactions and force transmission properties remains uncharted. Understanding the role of molecular interactions—such as motor protein properties, cross-linking agents, and steric interactions—in determining the long-range force transmission is crucial for advancing our knowledge and unlocking potential applications of cellular processes such as cell organization, force generation, and tissue morphogenesis.[26, 27]

In this study, we use light-controlled active matter to probe microscopic interactions that determine the length scale of force propagation in motor filament active matter.[25] We demonstrate that the microtubule length distribution controls a transition between the local force dissipating phase and the global force propagation phase. Through simulation and theory, we show that a small population of long microtubules is sufficient to induce long-range force transmission. By controlling the transition between force dissipation and propagation, we enable the modulation of active-matter-powered material transport and manipulation. This fine-tuned control over force transmission opens the door for light-controlled active matter-based cell sorting applications and innovative approaches to study and manipulate cellular events.

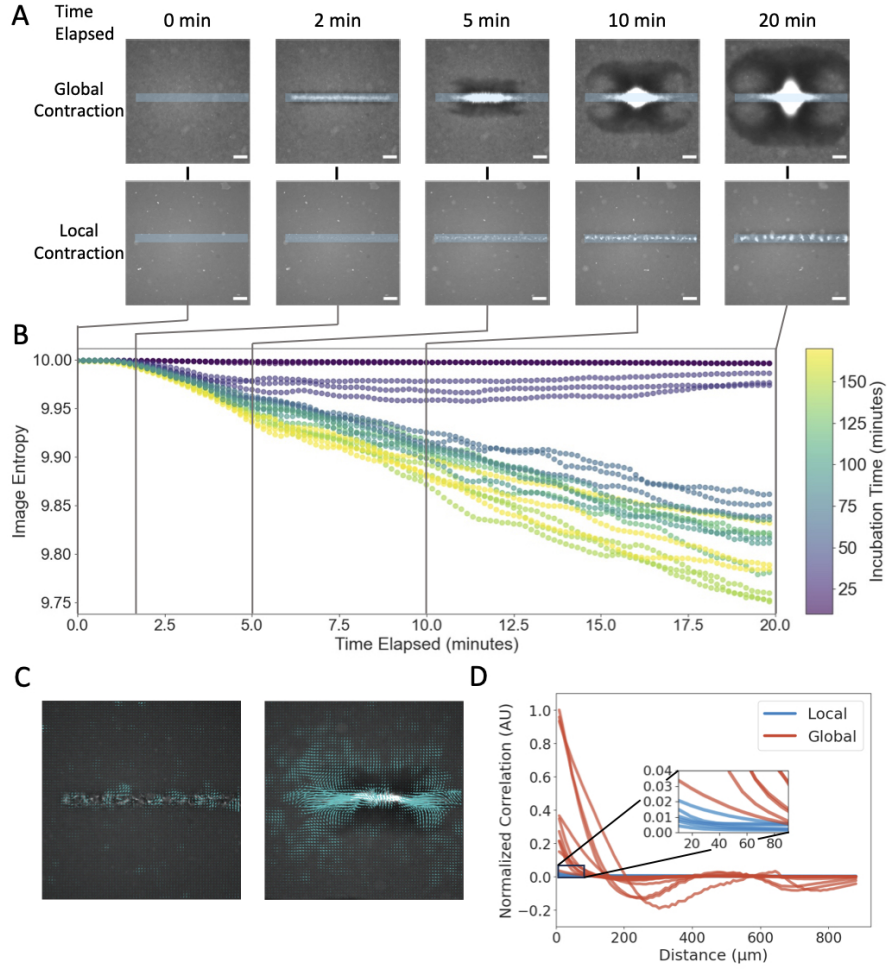


Fig. 1 Microtubule incubation induced phase transition between local to global organizations. **A**, Images of labelled microtubules during aster assembly in global phase(top) and local phase (bottom). Scale bar, 100 μm **B**, corresponding image entropy versus time. and corresponding plots of the image spatial standard deviation versus time. **C**, Representative of velocity vectors for PIV. Left: local phase. Right: global phase. **D**, Correlation distance computed from PIV. Inset shows local phase exhibit low correlation.

Main

Active matter incubation time switches contraction between the global force-propagating phase and the local force-dissipating phase.

During the cycles of growth, reconfiguration, and division, cells switch their internal cytoskeletal networks between phases of long-range and short-range organization

through modulation of the length and bundling effect of microtubules. To investigate the transition between force-dissipating and force-propagating properties of the two cytoskeletal organizations, we used a defined and optically controlled in vitro experimental system composed of stabilized microtubules and engineered kinesin motor proteins. Our microtubule kinesin active matter system consists of stabilized microtubules labeled with fluorophore and kinesin motor proteins fused with optically dimerizable iLID (improved light-induced dimer) proteins[25]. Upon light activation, the kinesin protein dimerization induces interactions between kinesins and neighboring microtubules, which leads to microtubule network formation and contraction into asters. In previous work, we observed that the pre-incubation of motors and microtubules prior to light activation could induce a transition between a long-range force propagating phase of the organization and a short-range force dissipating phase of the organization. Therefore, we performed a systematic study of system organization while quantitatively varying the duration of motor-microtubule incubation time.

Using the light-controlled system, we examined the role of pre-incubation time on cytoskeletal network phase by varying the incubation time of the microtubules and motor proteins in active matter system prior to light activation. In the experiments, we incubated the microtubules and motor proteins for a fixed period of time prior to activation, and then we light-activated a $25\text{ }\mu\text{m}$ by $800\text{ }\mu\text{m}$ rectangular region and monitored the resulting organization and contraction of the microtubule network as well as the induced fluid flow field using imaging and image analysis (Figure 1a). For a short pre-incubation time of 50 minutes or less, we observed a short-range phase with self-organized microtubule structures much smaller than the light pattern, at around $50\text{ }\mu\text{m}$. However, for incubation times greater than 50 minutes, we observed a long-range global phase where all the microtubules contract at the geometric center of the light pattern, forming structures that can span up to $800\text{ }\mu\text{m}$. Noticeably, for the short-range phase, very few microtubules outside of the light-activated region were incorporated into the self-organized asters, whereas in the global phase, microtubules over 300 microns away were persistently recruited into the aster throughout light-activated in the long-range global phase.

We found that the global phase of contraction can effectively concentrate and transport microtubules over $400\text{ }\mu\text{m}$. We used image entropy, which measures the randomness or uniformity within the microtubule distribution (Figure 1b). In the context of our experiments, it quantifies the uniformity of the microtubule distribution. A higher entropy value indicates a more random and uniform distribution of microtubules, while a lower entropy value suggests a more organized and concentrated distribution of microtubules. Initially, both phases exhibit an image entropy near the maximum of 10 bits, implying a predominantly random distribution of microtubules. We observed a decrease in entropy to 9.75 occurs in the global phase due to the effective contraction and transport of microtubules, which results in differential concentration of microtubules. Furthermore, microtubules outside of the light-activated regions were recruited into the aster due to vortices and fluid flows generated in the global phase. This contrasts with the local phase, where the image entropy remains close to 10 bits, indicating no significant change in the distribution pattern of microtubules except for short-range organization within the light-activated region. The decrease in entropy of

the global phase of contraction shows the ability to transport microtubules and materials over 400 μm , whereas the local phase of contraction fails to transport microtubules over 50 μm .

We measured the velocity field of the microtubule network using particle imaging velocimetry (PIV). The velocity correlation quantifies the degree to which the speeds and directions of particles are synchronized across the microtubule network, providing insight into the coherent or disparate movement behaviors over space (Figure 1c). The absolute magnitude of velocity fields increased by 100 folds as the active matter system transitioned from the local force-dissipating phase to the global force-propagating phase (Figure 1d). Within the global force-propagating phase, the normalized correlation of velocity peaks at one and undergoes a sign change at a distance of 100 μm , mirroring half of the dimensions of contracted asters. This pronounced correlation of velocity vectors in the global phase signifies the propagation of forces across extensive spans, with velocity vectors maintaining their magnitude and direction over several hundred microns. This behavior underscores the phase's potential utility in leveraging its force-propagation capabilities for material transport applications. Conversely, the phase dominated by short-range force dissipation exhibits a peak velocity correlation of 0.02 and maintains a value near zero. There is also no sign change in the correlation due to the insignificant magnitude of the velocity vectors. The highly correlated and synchronized velocity fields demonstrate the force propagation ability in the global phase, and the weakly aligned velocity fields show the forces were dissipated in the local phase.

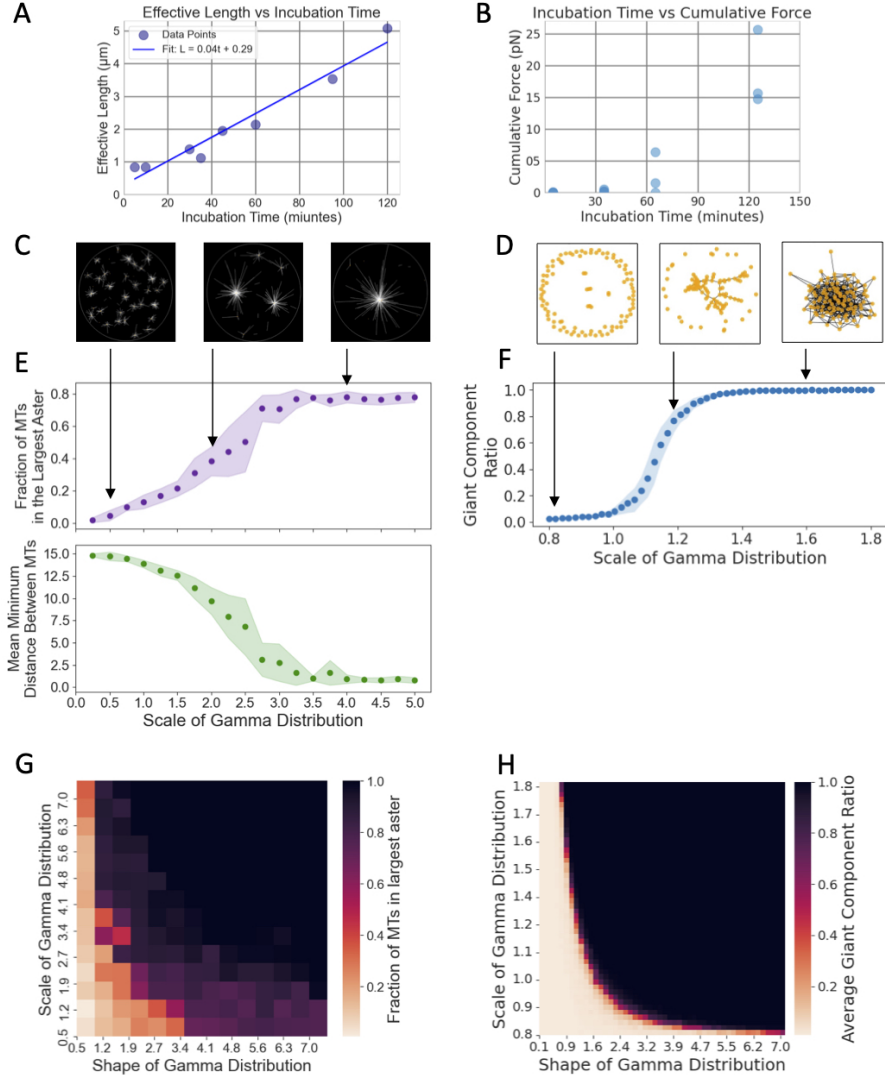


Fig. 2 A fivefold increase in microtubule bundle length enables force propagation phase in active networks.. **A**, Incubation time increases microtubule effective length by 5 folds over 120 minutes **B**, Active matter system exert close to 100 times more force after incubation by moving polystyrene tracer beads. **C**, Images of Cytosim simulation under different conditions. **D**, Images of percolation simulation under different conditions. **E**, The top plot shows the fraction of microtubules in the largest aster versus the scale parameter of the gamma distribution. The bottom plot shows the mean of the minimum distance between each pair of microtubules versus the scale parameter of the gamma distribution. **F**, Giant component ratio vs scale of gamma distribution for the percolation simulations. **G**, Heatmap showing the relationship of the shape and scale of gamma distributed microtubule species and fraction of microtubules in the largest aster. **H**, Heatmap showing the relationship of the shape and scale of gamma distributed edge species and the giant component ratio.

Increases in microtubule length induce a percolation transition.

To elucidate the microscopic mechanism underlying the transition from the local force-dissipating phase to the global force-propagating phase, we performed fluorescence recovery after photobleaching (FRAP) experiments. FRAP allows for the measurement of the effective length of microtubule structures from the diffusion coefficient of the recovery of fluorescent microtubules after photobleaching a specific region. We found that the length of the microtubule structures increased linearly from $0.9\text{ }\mu\text{m}$ to $5\text{ }\mu\text{m}$ over a period of 2 hours, with a rate of $2.05\text{ }\mu\text{m/hr}$ (Figure 2a). This rate of increase is 4 times higher than the GMP-cpp (Material and Methods) polymerization rate of tubulin, which is $0.5\text{ }\mu\text{m/hr}$ [28–30]. GMP-cpp is a slowly hydrolyzable analog of GTP that stabilizes microtubules, and its polymerization rate serves as a reference for the observed growth rate. Thus, the higher growth rate observed in our experiments suggests that microtubules exhibit bundling behavior, which increases the length of each microtubule structure by 5-fold in 120 minutes.

To test the material transport capability of the contractions, we placed $10\text{ }\mu\text{m}$ polystyrene tracer beads in the system and recorded their movements. The tracer beads underwent Brownian motion for incubation times of 0 to 30 minutes, indicating that the active matter system could not exert significant forces on the cargo. However, after incubating the system for more than 60 minutes, the contraction moved the tracer beads by up to $200\text{ }\mu\text{m}$, and the cumulative force exerted on the beads increased by up to 25-fold to 26 pN (Figure 2b). The cumulative force was calculated by analyzing the displacement of the beads and using Stokes’ law to estimate the force required to overcome the drag in the medium. The directed movement of the tracer beads demonstrates that bundled microtubules drive the global force-propagating phase, exhibiting material transport and long-range order.

To validate the microtubule-bundling-induced transition between the local force-dissipating phase and the global force-propagating phase, we first employed Cytosim, a numerical simulation platform designed to model cytoskeletal mechanics by simulation each microtubule and kinesin (Figure 2c) [29]. We investigated whether increasing the length of the microtubules would cause the system to transition from having many local asters to having a global aster. The length of the microtubules was modeled using a modified gamma distribution, where the shortest microtubule was $1\text{ }\mu\text{m}$, and the longest was $25\text{ }\mu\text{m}$ [31]. We fixed the total length of all microtubules to $1000\text{ }\mu\text{m}$ to simulate bundling instead of spontaneous polymerization of free tubulin. As we increased the scale parameter, which introduced a small portion of long microtubules, the simulated active matter system transitioned from having many local asters to having a global aster. When the scale parameter of the microtubule length distribution increased to 2.75, with an average microtubule length of $3.7\text{ }\mu\text{m}$, we observed plateaus in both the fraction of microtubules in the largest aster and the mean distance between any pair of microtubules, indicating the system’s transition into the global phase (Figure 2e). Increasing either or both the shape parameter, which primarily influences the peak of the length distribution, and the scale parameter, which primarily influences the spread of the length distribution, caused the simulated system to transition from the local phase with many local asters to the global phase

where most of the microtubules are in one aster (Figure 2g). Our numerical simulation validates our experimental observation that as the microtubule length increases, the active matter system transitions from the local to the global phase.

To further validate the phase transition, we developed a more generalized network-based simulation rooted in percolation theory (Figure 2d). Percolation theory describes the formation of connected clusters in a random graph and has been applied to study phase transitions in various systems[32]. In our network-based simulation, instead of explicitly representing each microtubule and kinesin, we abstracted the system into nodes, representing the center of mass of microtubules, and edges, symbolizing potential connections between them. The edge probabilities, reflecting the likelihood of interaction based on the relative lengths and spatial orientations of the microtubules, were determined using the same gamma distribution as in the Cytosim simulation. We first explored varying the scale parameter while keeping the shape parameter at 1. As we increased the scale parameter, we observed an exponential increase in the size of the largest connected component, followed by a plateau where all the nodes became connected to each other (Figure 2f). When increasing both the scale and shape parameters, the simulated system exhibited a transition from the disconnected phase to the connected phase with a giant component, resembling a percolation transition (Figure 2h). This phase transition in the network-based simulation validates the microtubule-bundling-mediated local force-dissipating to the global force-propagating phase transition observed in the experimental system. Furthermore, our simulations hint at the influential role of MT length distribution in facilitating spatial dynamics within the cytoskeleton. This aligns with the observed load-bearing attributes of microtubule networks, attributed to their lateral interactions with other filaments and molecular structures [33].

The global force propagating phase enables persistent material transport

To study the long-range interactions enabled by the global force-propagating phase of the active cytoskeleton network, we constructed an aster merger operation (Figure 3a) where we connected two asters using light patterns, as previously described by[25]. In both the local and global phases, two asters were formed by circular light-excitation patterns, with the local phase aster being smaller and depleting less material compared to the global phase aster. Upon connecting the pair of asters using a rectangular pattern with a high aspect ratio, we observed that in the global phase, the two asters merged after a short delay time (~ 1 minute), while the aster pair in the local phase did not exhibit any movement. These findings further reinforced that the moving and merging global phase asters are dynamic and constantly remodeling, whereas the local phase asters are closer to steady-phase structures[34].

The ability to direct aster formation and movement, both spatially and over time, marks a critical progression toward transport applications using the active cytoskeleton network. By confining the active network in the global phase using microfabricated chambers or microfluidic devices, we demonstrated the simultaneous movement of multiple asters using multiple dynamic light patterns (Figure 3b). As asters moved, inflows of microtubule bundles emerged within the light pattern, feeding into and pulling the

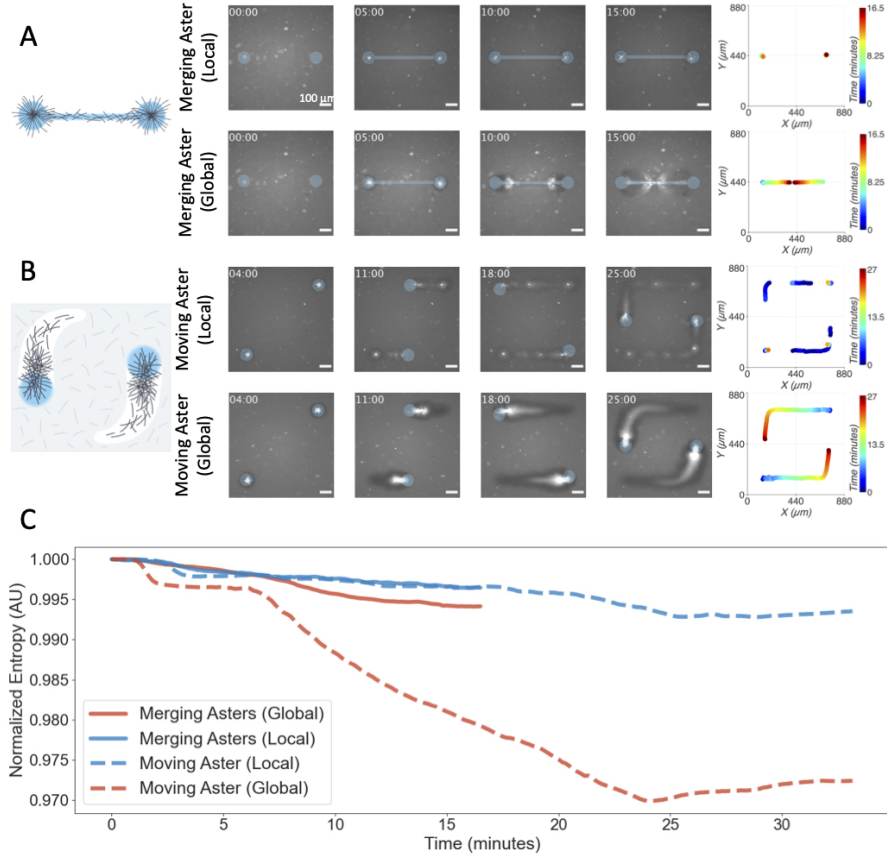


Fig. 3 Force propagation driven by global contraction enables material transport. A, Aster linking in both local and global condition. **B,** Aster moving in both local and global condition. **C,** Image entropy of experiments in A and B. All scale bar, 100 μm

aster. Concurrently, outflows, resembling comet-tail streams, trailed the moving asters. During the aster movement, the global phase asters followed the dynamic light patterns without interruption. In contrast, local phase asters struggled to match the pace of the light patterns, often leading to transient and static asters that subsequently gave rise to new aster formations along the light pattern's path.

We characterized the merging and moving aster operations under different phases using image entropy calculations, as described earlier (Figure 3c). Operations conducted in the global phase instigated more substantial material displacements, correlating with rapidly decreasing entropy levels. In comparison, local phase operations caused limited material flow and microtubule-depleted areas, resulting in only slightly reduced entropy values. These observations resonate with simulation insights, which suggest that a more interconnected active cytoskeleton network, characteristic of the global phase, offers enhanced support, allowing microtubules to withstand

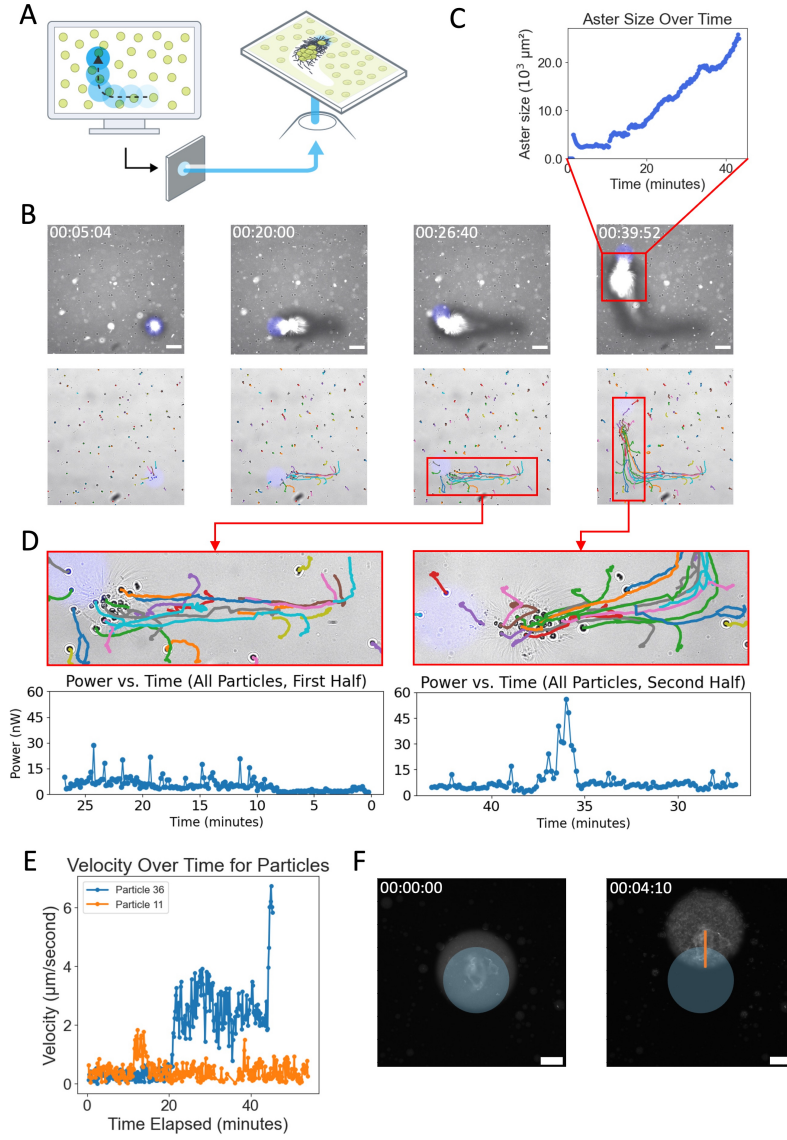


Fig. 4 Aster-based active cell transport. **A**, Schematics of cell transport use active matter. **B**, Time-lapsed images of using aster to concentrate and transport Jurkat T cells. Scale bar, 100 μm. **C**, Aster size increases as aster displacement increases. **D**, Power generated by moving cells with respect to time. **E**, Example of cell velocity of a stationary cell (orange) vs a cell captured by the aster (blue). **F**, Proof of concept motile droplet powered by contracting active cytoskeleton. Scale bar, 100 μm.

forces and facilitate material transportation. In contrast, the less interconnected local phase network results in limited material transport and force propagation.

Force propagating active matter powers cell transporter and droplet motility

The ability of the active network to generate force and transport materials indicates its potential to serve as an engine and transport agent for biological processes and future bio-robots. To demonstrate the transport ability of biological materials, we explored the moving of cells in suspension. The setup consists of human Jurkat cells in suspension in the active cytoskeleton network. Upon light activation, the contracting global phase aster picked up the cells. By using dynamic light patterns similar to the previous demonstration (Figure 4a), we were able to direct the aster to move for 1 mm while picking up cells along the movement path (Figure 4b). As the global phase aster moves, the cross-section area of the aster increases linearly (Figure 4c), which aids in retaining the cell it is transporting. As the aster moves into proximity to a cell, the inflows exert from 10 to 50 nW to pull the cells into the aster (Figure 4d). The global phase aster is also capable of capturing multiple cells simultaneously. At the beginning of the experiment, the global phase aster was only able to capture cells within the light-activated region. As the incubation time and also the aster size increased, material outside of the light-activated region was rapidly recruited, hence increasing the range the aster could capture cells. Out of 32 cells captured, the global phase aster failed to retain 2 cells throughout the entire movement. The two cells that were released from the "arms" of the aster and cells in the core of the aster were all transported throughout the entirety of the experiment. This showed that the "arms" and the "core" of the aster potentially have different structures, and the "core" might have more carrying capacity due to the randomly crosslinked structure compared to the "arms", which have a more nematic structure. Cells that were not captured by the global phase aster show little movement (Figure 4e) compared to captured cells. In the biological context, the cytoskeleton and the active fluids generated by it have been proposed to lead to the emergence of cytoplasmic streaming, which can enhance cellular transport. To mimic this biological process, we encapsulated our active cytoskeleton network in aqueous droplets emulsified in oil. When activated by light, the active cytoskeleton network did not seem to propel the aqueous droplet in either the global phase or the local phase (Figure 4f). However, outside of our current defined phases, we were able to generate directed movement of the droplet by light activation, and the movement quickly stopped when we turned off the activation. In this phase, the active network does not contract into global or local asters but exhibits a highly crosslinked state with minimal contraction. We hypothesize that the crosslinked network created a local divergent at the water-oil interface, which resulted in Marangoni flow and propelled the droplet forward.

Summary and Outlook

Here, we demonstrated the microtubule-bundling-induced transition from the local force-dissipating phase to the global force-propagating phase of active cytoskeleton networks. A 5-fold increase in the average microtubule length results in the transition from a local contraction phase with disordered and low magnitude velocity to a global contraction phase with a 100-fold increase in the distance and a 20-fold increase in

the magnitude over which forces propagate. The global phase generates 10pN forces that enable material transport over hundreds of micrometers.

Our results reveal an important role for microtubule bundle length in determining transitions between local and global contractile states. Our findings, validated by both numerical and network-based simulations, suggest that even a few elongated microtubules can significantly promote the shift from the local to the global phase of the organization. This concept is not only foundational for understanding active matter but could have broader implications for self-organization in various systems. Using light patterns, we discovered the active cytoskeleton network’s potential for long-range material transport in the global force-propagating phase, in contrast to the relatively static behavior observed in the local force-dissipating phase. Our findings enable new directions in understanding and manipulating active matter systems, especially in the realm of biological processes and applications. With the global phase of the active cytoskeleton network displaying potential for material transport and long-range interactions, there’s a tangible avenue for advancements in biological and perhaps even medical applications. We have successfully demonstrated the ability of our active cytoskeleton network to transport cells over millimeter-scale distances, induce physical stress on cells, and move droplets in a directed fashion. Implementing our light-controlled active network with membranes and confinements such as vesicles can pave the way for innovations in bio-manufacturing, with each confined network performing different tasks and communicating for biological or chemical production.

The study also offers a stepping stone towards a deeper comprehension of the self-organization in biological systems. By understanding how modifications in microtubule bundling can have large-scale effects on network contraction, researchers could further probe into natural systems’ inherent ability to self-organize and communicate across multiple spatial and temporal scales. This knowledge could be transformative in fields like neuroscience and developmental biology, where we could study how connected components like microbes and neurons communicate and form dynamic structures. In material science, self-assembling and self-organizing materials have long been recognized for their unique properties and applications. The principles uncovered in this study could inspire the design of novel synthetic materials that can transition between local and global states, enabling programmable material properties and functions. In conclusion, our work not only provides a fundamental understanding of the role of microtubule bundling in the transition between local and global contractile states in active matter systems but also opens up exciting possibilities for future research and applications in biology, medicine, and material science.

References

- [1] Huxley, H., Hanson, J.: Changes in the cross-striations of muscle during contraction and stretch and their structural interpretation. *Nature* **173**(4412), 973–976 (1954)
- [2] Huxley, A.F., Niedergerke, R.: Structural changes in muscle during contraction; interference microscopy of living muscle fibres. *Nature* **173**(4412), 971–973 (1954)

- [3] Gittes, F., Mickey, B., Nettleton, J., Howard, J.: Flexural rigidity of microtubules and actin filaments measured from thermal fluctuations in shape. *J. Cell Biol.* **120**(4), 923–934 (1993)
- [4] Mitchison, T., Kirschner, M.: Dynamic instability of microtubule growth. *Nature* **312**(5991), 237–242 (1984)
- [5] Lauffenburger, D.A., Horwitz, A.F.: Cell migration: a physically integrated molecular process. *Cell* **84**(3), 359–369 (1996)
- [6] Shelley, M.J.: The dynamics of microtubule/motor-protein assemblies in biology and physics. *Annu. Rev. Fluid Mech.* **48**, 487–506 (2016)
- [7] Theurkauf, W.E.: Premature microtubule-dependent cytoplasmic streaming in cappuccino and spire mutant oocytes. *Science* **265**(5181), 2093–2096 (1994)
- [8] Gutzeit, H.O., Koppa, R.: Time-lapse film analysis of cytoplasmic streaming during late oogenesis of drosophila. *Development* **67**(1), 101–111 (1982)
- [9] Theurkauf, W.E., Smiley, S., Wong, M.L., Alberts, B.M.: Reorganization of the cytoskeleton during drosophila oogenesis: implications for axis specification and intercellular transport. *Development* **115**(4), 923–936 (1992)
- [10] Howard, J.: *Mechanics of Motor Proteins and the Cytoskeleton*, New edition edn. Sinauer Associates is an imprint of Oxford University Press, ??? (2001)
- [11] Heisenberg, C.-P., Bellaïche, Y.: Forces in tissue morphogenesis and patterning. *Cell* **153**(5), 948–962 (2013)
- [12] Oakes, P.W., Banerjee, S., Marchetti, M.C., Gardel, M.L.: Geometry regulates traction stresses in adherent cells. *Biophys. J.* **107**(4), 825–833 (2014)
- [13] Heald, R., Tournebise, R., Habermann, A., Karsenti, E., Hyman, A.: Spindle assembly in xenopus egg extracts: respective roles of centrosomes and microtubule self-organization. *J. Cell Biol.* **138**(3), 615–628 (1997)
- [14] Biswas, A., Kim, K., Cojoc, G., Guck, J., Reber, S.: The xenopus spindle is as dense as the surrounding cytoplasm. *Dev. Cell* **56**(7), 967–975 (2021)
- [15] Desai, A., Murray, A., Mitchison, T.J., Walczak, C.E.: Chapter 20 the use of xenopus egg extracts to study mitotic spindle assembly and function in vitro. In: Rieder, C.L. (ed.) *Methods in Cell Biology* vol. 61, pp. 385–412. Academic Press, ??? (1998)
- [16] Gard, D.L.: Microtubule organization during maturation of xenopus oocytes: assembly and rotation of the meiotic spindles. *Dev. Biol.* **151**(2), 516–530 (1992)
- [17] Abercrombie, M., Heaysman, J.E., Pegrum, S.M.: The locomotion of fibroblasts

- in culture. II. “RRuffling”. *Exp. Cell Res.* **60**(3), 437–444 (1970)
- [18] Li, Y., Kučera, O., Cuvelier, D., Rutkowski, D.M., Deygas, M., Rai, D., Pavlovič, T., Vicente, F.N., Piel, M., Giannone, G., Vavylonis, D., Akhmanova, A., Blanchoin, L., Théry, M.: Compressive forces stabilize microtubules in living cells. *Nat. Mater.* **22**(7), 913–924 (2023)
 - [19] Goldstein, R.E., Meent, J.-W.: A physical perspective on cytoplasmic streaming. *Interface Focus* **5**(4), 20150030 (2015)
 - [20] He, L., Wang, X., Montell, D.J.: Shining light on drosophila oogenesis: live imaging of egg development. *Curr. Opin. Genet. Dev.* **21**(5), 612–619 (2011)
 - [21] Bastock, R., St Johnston, D.: Drosophila oogenesis. *Curr. Biol.* **18**(23), 1082–7 (2008)
 - [22] Stein, D.B., De Canio, G., Lauga, E., Shelley, M.J., Goldstein, R.E.: Swirling instability of the microtubule cytoskeleton. *Phys. Rev. Lett.* **126**(2), 028103 (2021)
 - [23] Sanchez, T., Chen, D.T.N., DeCamp, S.J., Heymann, M., Dogic, Z.: Spontaneous motion in hierarchically assembled active matter. *Nature* **491**(7424), 431–434 (2012)
 - [24] Nédélec, F.J., Surrey, T., Maggs, A.C., Leibler, S.: Self-organization of microtubules and motors. *Nature* **389**(6648), 305–308 (1997)
 - [25] Ross, T.D., Lee, H.J., Qu, Z., Banks, R.A., Phillips, R., Thomson, M.: Controlling organization and forces in active matter through optically defined boundaries. *Nature* **572**(7768), 224–229 (2019)
 - [26] Sanchez, C., Arribart, H., Guille, M.M.G.: Biomimetism and bioinspiration as tools for the design of innovative materials and systems. *Nat. Mater.* **4**(4), 277–288 (2005)
 - [27] Whitesides, G.M.: Bioinspiration: something for everyone. *Interface Focus* **5**(4), 20150031 (2015)
 - [28] Hilitski, F., Ward, A.R., Cajamarca, L., Hagan, M.F., Grason, G.M., Dogic, Z.: Measuring cohesion between macromolecular filaments one pair at a time: depletion-induced microtubule bundling. *Phys. Rev. Lett.* **114**(13), 138102 (2015)
 - [29] Nédélec, F., Foethke, D.: Collective langevin dynamics of flexible cytoskeletal fibers. *New J. Phys.* **9**(11), 427 (2007)
 - [30] Najma, B., Baskaran, A., Foster, P.J., Duclos, G.: Microscopic interactions control a structural transition in active mixtures of microtubules and molecular motors (2023)

- [31] Odde, D.J., Cassimeris, L., Buettner, H.M.: Kinetics of microtubule catastrophe assessed by probabilistic analysis. *Biophys. J.* **69**(3), 796–802 (1995)
- [32] Artime, O., De Domenico, M.: Percolation on feature-enriched interconnected systems. *Nat. Commun.* **12**(1), 2478 (2021)
- [33] Brangwynne, C.P., MacKintosh, F.C., Kumar, S., Geisse, N.A., Talbot, J., Mahadevan, L., Parker, K.K., Ingber, D.E., Weitz, D.A.: Microtubules can bear enhanced compressive loads in living cells because of lateral reinforcement. *J. Cell Biol.* **173**(5), 733–741 (2006)
- [34] Surrey, T., Nédélec, F., Leibler, S., Karsenti, E.: Physical properties determining self-organization of motors and microtubules. *Science* **292**(5519), 1167–1171 (2001)